Food Research International 162 (2022) 112046

Contents lists available at ScienceDirect

Food Research International

journal homepage: www.elsevier.com/locate/foodres

NMR-based metabolomics reveals the antibacterial effect of electrolysed water combined with citric acid on *Aeromonas* spp. in barramundi (*Lates calcarifer*) fillets

Leijian Chen [a], Xuan Li [a], Xiaowei Lou [a,b], Weichen Shu [a], Yaowen Hai [a], Xiaokang Wen [a], Hongshun Yang [a,b,*]

[a] Department of Food Science and Technology, National University of Singapore, Singapore 117542, Singapore
[b] National University of Singapore (Suzhou) Research Institute, 377 Lin Quan Street, Suzhou Industrial Park, Suzhou, Jiangsu 215123, PR China

ARTICLE INFO

Keywords:
Cell membrane
Spoilage microorganism
Barramundi
NMR
Food omics
Electrolyzed water
Organic acid
Fish

ABSTRACT

The citric acid (CA) and electrolysed water (EW) are considered effectively in inactivating microorganisms. The objective of this study was to explore the bactericidal mechanism of CA combined with EW on *Aeromonas* spp. in barramundi (*Lates calcarifer*) by in vitro metabolomics method. This study determined the survival population of three strains of *Aeromonas* bacteria (strain 1: *Aeromonas salmonicida* strain A1 (skin); strain 2: *A. veronii* strain Til2 (gut), and strain 3: *A. hydrophila* strain B11 (gill)), which were isolated and identified from putrid barramundi treated alone or in combination with 1 % CA and EW (free available chlorine (FAC) 25 mg/L, pH 3.23, oxidation-reduction potential (ORP) 1015 mV). The bactericidal mechanism was investigated by microbiological analysis, nuclear magnetic resonance (NMR), multivariate data analysis, and fluorescence staining analysis. The results showed that the combined treatment significantly reduced the number of *Aeromonas* bacteria at 1.64–1.69 log CFU/g and extended the shelf life of barramundi fillets. In addition, the combined treatment had a higher effect on the cell membrane integrity of the bacteria. In total, 36 metabolites were identified in the three strains. The undissociated molecules of CA can enter the cytoplasm, resulting in cell damage and inhibiting metabolic pathways. EW could lead to the reduction of metabolic products caused by oxidative stress and acid stress. Under the synergistic stress of CA and EW, the changes of main metabolite contents in the combined treatment group were significantly reduced. After combined treatment, there were 20, 31, and 31 pathways in which carbohydrate metabolism, amino acid metabolism, and energy metabolism were changed considerably. These findings indicated that the bactericidal mechanism of the bactericidal substance might be explained by the interference of the metabolic pathway, which guided post-treatment sanitisation and extended the applicability of the NMR spectrum to specific spoilage organisms (SSO) analysis in fish.

1. Introduction

Barramundi (*Lates calcarifer*), also known as Asian bass across the Asia-Pacific area, is a significant food fish in the tropics, with an annual worldwide output of roughly 164,000 t, 40 % of which is produced in captivity (FAO, 2012). However, barramundi muscles are sensitive to degradation due to biochemical features such as highly soluble nitrogen compounds, a relatively high unsaturated lipid content, and a low collagen concentration that promote autolysis and fast microbial multiplication (Truong, Buckow, Nguyen, & Nguyen, 2021). Microbial activity is responsible for losing a quarter of the world's food supply and 30 % of the captured fish. Numerous *Aeromonas* species are found in the aquatic environment and are identified as spoilage organisms in seafood, primarily tropical or warm-water fish and crustaceans (Hoel, Vadstein, & Jakobsen, 2019). *Aeromonas* isolates produced mucus, with 95 % exhibiting lipase and protease activity (Arslan & Küçüksari, 2015). While the spoilage potential is determined by its capacity to create metabolites associated with product deterioration (Iulietto, Sechi, Borgogni, & Cenci-Goga, 2015), identifying the actual spoilage potential involves a mix of sensory, microbiological, and chemical studies (Zhao et al., 2017). Many *Aeromonas* species have been identified as part of the seafood spoilage microbiota, but little is known about the metabolites

* Corresponding author at: Department of Food Science and Technology, National University of Singapore, Singapore 117542, Singapore.
E-mail address: fstynghs@nus.edu.sg (H. Yang).

https://doi.org/10.1016/j.foodres.2022.112046
Received 29 May 2022; Received in revised form 3 October 2022; Accepted 10 October 2022
Available online 17 October 2022
0963-9969/© 2022 Elsevier Ltd. All rights reserved.

generated by *Aeromonas* spp. growth in varied seafood.

Chemical sanitisers such as essential oils and organic acids are often employed in the food business, as are non-chemical treatments such as ultrasound and UV light. Combining several sanitisation procedures may result in synergistic or additive antibacterial effects that are often superior to those achieved alone. Citric acid (CA), also known as the tricarboxylic acid ($C_6H_8O_7$), is a widely used preservative, acidifier, flavouring agent, emulsifier, isolator, and buffer in a variety of sectors, including food, beverages, pharmaceuticals, and cosmetics (Cho & Ha, 2021). CA has potent antiviral and sanitisation properties and could permanently interfere with virus replication (Koromyslova, White, & Hansman, 2015, Eliuz, 2020). In addition, its ecologically friendly characteristics and its good physical and chemical structure make it an excellent candidate for culinary, cosmetic, and pharmaceutical applications. EW is mainly sterilised by hypochlorous acid, primarily through oxidative damage to harmful bacteria and degradation of bacteria's cell membranes (Dewi, Stanley, Powell, & Burke, 2017, Meireles, Giaouris, & Simões, 2016). Several research investigations have been carried out in vitro studies using cell suspensions demonstrating that EW may kill pathogens and spoilage organisms such as *Listeria monocytogenes*, *Escherichia coli, Salmonella*, *Vibrio parahaemolyticus*, and *Pseudomonas aeruginosa*, among others (Kim, Tango, Chelliah, & Oh, 2019, Liu, Lan, Wang, & Xie, 2022).

The overall objective of this study was to explore the bactericidal mechanism of CA combined with EW (FAC 25 mg/L) on *Aeromonas* spp. in barramundi by in vitro metabolomics method. This study may help provide the additional scientific basis for adding combined treatment steps in the anti-spoilage of seafood by revealing the metabolic changes of bacteria in the antibacterial process and extending the applicability of the NMR spectrum to SSO analysis in fish storage.

2. Methodology

2.1. Materials

EW was produced in an electrolysis apparatus using a 0.9 % sodium chloride solution (Hoshizaki, ROX-10WB3, Hoshizaki Singapore Pte Ltd, Singapore). The FAC concentration was determined using colourimetric test strips (Merck, Singapore). The ORP concentration was determined by ORP meter (HM Digital ORP-200, Culver City, CA, USA). The pH was determined using a pH meter (Thermo Orion pH meter, Waltham, MA, USA). sodium 3-trimethylsilyl [2,2,3,3-d4] propionate (TSP), phosphate-buffered saline (PBS, pH 7.2). CA powder, Luria-Bertani (LB) broth, *Aeromonas* Isolation Agar, peptone water, and LB agar were purchased from Sigma-Aldrich (Singapore). Becton, Dickinson, and Company (Sparks, MD, USA) supplied the neutralising buffer.

EW was collected in a sterile glass container and utilised to prevent chorine loss within 1 h of manufacture. EW was diluted with sterilised deionised water (DW) to achieve a FAC concentration of 25 mg/L (ORP 1015 ± 26.8 mV, pH 3.23 ± 0.2). EW was initially quantified semi-quantitatively by comparing the test strip to a colour scale to assess FAC. After the test strip was immersed in diluted EW for 2 s, it was immediately placed into the Reflectoquant strip adapter for quantitative reading. The 1 % CA solution was obtained by mixing CA powder with DW in 1 % W/V ratio. The 1 % CA and EW combination solution was obtained by ultrasonic treatment for 15 min after completely mixing CA powder with EW in 1 % w/v ratio. The FAC of the combination solution was tested and controlled at 25 mg/L.

2.2. Bacterial strain isolation, identification, and culture conditions

A barramundi (*Lates calcarifer*), which weighs around 1000 ± 100 g on average, was bought at the local supermarket (Sheng Siong) in Singapore. The fish was gutted and transferred to the laboratory within 1 h in an icebox. The gills, intestines, and fish skin were divided and put into separate containers and kept separately at 4 °C until putrefaction smells emerged. A 10 ± 0.1 g sample of each component of fish was homogenised for 90 s in 90 mL of 0.1 % peptone water (W/V) by a stomacher (Masticator Stomacher, IUL Instruments, Germany). After dissolution in peptone water, 100 μL samples were cultured on *Aeromonas* isolation agar for 24 h at 37 °C. Subsequently, single colonies were isolated for morphological characteristics, and isolates with similar morphology to *Aeromonas* spp. were selected. In order to find different types of isolates, isolates with similar colony morphology were removed. After removing similar isolates, samples were obtained for further inspection. Individual colonies were cut together with LB agar and then stored under refrigeration at 4 °C before being subjected to molecular identification.

As for molecular identification, bacterial DNA was extracted using the GenElute™ bacterial genomic DNA kit. Each colony was added 100 μL extract, incubated at 95 °C for 10 min, and then added 100 μL diluent. After that, the PCR purification was performed using a Favorgen gel / PCR purification kit (300 prep) and directly loaded 2 μL of extracted gDNA products onto the gel using exTEN Mastermix (1st BASE). Then bacterial DNA sequences (primer: 27F and 1492R) were obtained by sanger sequencing. The 27F and 1492R sequences were cut using Chromas software. DNAMAN software was used to assemble the sequence, and then the assembled sequence was imported into NCBI nucleotide BLAST and picked the top 10 hit results for the report.

After molecular identification, the selected strains (Three species of *Aeromonas* strains) were stored at −80 °C, and the strains were activated at 37 °C in 5 mL sterile LB broth for 24 h before use. A loop of cell suspension was streaked on the LB agar and cultured at 37 °C for 24 h to separate a single colony. Each colony was injected into 10 mL LB broth, subcultured twice for 24 h at 37 °C, and then centrifuged at 8000*g* (about 8 log CFU/mL) for 10 min at 15 °C. The resultant tray was cleaned twice with 10 mL of peptone water and then resuspended and washed before centrifugation (8000*g*, 10 min, 15 °C). Then the cells were washed and suspended in 10 mL of peptone water. Finally, the obtained suspension was diluted (V/V = 1/10) to about 8 log CFU/mL to prepare for future inoculation operations.

2.3. Preparation of sterilised fish fillets

Sterile fish fillets were produced as described by Lou, Zhai, and Yang (2021) with slight modifications. First, the skin and intestinal mucosa were cleansed with sterile distilled water. Next, mucus from the body surface and intestinal cavity should be removed twice with 5 % Na_2CO_3 solution. Next, each side of the fish was immersed for 3 min in a 2 % formalin solution. After that, scrubbed with 70 % ethanol and dry with sterile airflow. Finally, the skin of the fish was removed with a sterile disinfected knife and cutting board and then cut the fish into 10 ± 0.1 g fillets. After processing, the fish fillets were placed in a sterile petri dish, irradiated by ultraviolet light on both sides for 15 min, and stored at 4 °C (within 2 h) before use.

2.4. Inoculation of bacteria strains

The isolated strains were stored at − 80 °C and needed to be activated after being continuously transported twice for 6 d in 10 mL LB broth at 4 °C before use, then plated on LB agar to obtain discrete colonies. Next, the colonies were recultured in LB broth at 37 °C until the inoculum reached 8 log CFU/mL. The sterile fish fillet was immersed in the inoculum, and the final cell density reached about 6 log CFU/g. The inoculated fillets were dried under a stream of sterile air for 5 min (Yemmireddy, Cason, Moreira, & Adhikari, 2020). Then, each inoculated fillet was put in a sterile petri dish and placed in a biosafety cabinet. After 2 h of bacterial colonisation, the samples were removed for the sanitisation experiment.

2.5. Sanitising treatments

The inoculated barramundi was split into four treatment groups: (I) DW; (II) 1 % CA; (III) EW; and (IV) CA and EW combination. After 10 ± 0.1 g sample was immersed in the 40 mL treatment solution (25 °C) for 5 min, 50 mL of neutralisation buffer was added to neutralise residual chlorine and acidity and terminate sanitisation (Zhao et al., 2017). Next, the sanitisation effect of the different treatments on samples was analysed. After that, the remaining barramundi fillets were placed separately in the sterile petri dish and refrigerated at 6 °C for 6 days. At 0, 1, 2, 4, and 6 days, enumeration of *Aeromonas* spp. was conducted, and metabolite extraction was performed at 0, 4, and 6 days.

2.6. Enumeration of Aeromonas spp.

The enumeration of *Aeromonas* spp. for sanitising treatment analysis was conducted according to Wu, Zhao, Lai, and Yang (2021). First, barramundi fillets were homogenised with the 90 s in a neutralisation treatment solution (40 mL treatment solution and 50 mL neutralisation buffer), then tenfold dilution with 0.1 % peptone water and plating on LB agar with 100 μL diluent. As for the enumeration of *Aeromonas* spp. for six-day storage analysis, 10 g samples were taken out and mixed with 90 mL 0.1 % peptone water, then homogenised for 90 s in a stomacher (Masticator Stomacher, IUL Instruments, Germany). After that, tenfold dilution with peptone water and plated on LB agar with 100 μL diluent. Finally, after 24 h of incubation (37 °C), the cell population was quantified using log CFU/g barramundi cube.

2.7. Cell membrane integrity analysis

The propidium iodide (PI) uptake test was conducted as Wu et al. (2019) described with slight modifications. First, each *Aeromonas* strain was cultured for 24 h after inoculation at 37 °C. Then 5 mL bacterial liquid was taken out and centrifuged (8000*g*, 10 min, 4 °C). The supernatants were discarded, and the cells were rinsed with PBS at least 3 times. Next, the cells were resuspended in 10 mL sterile saline (0.85 %, w/v) supplemented with treatment solution (1 % CA, EW, CA + EW, and DW) and incubated at 37 °C for 4 h. After the solution was centrifuged (8000*g*, 10 min, 4 °C), the supernatants were discarded, and the cells were washed with PBS at least 3 times. Then, the cells were resuspended in a 5 mL PBS solution and added 0.3 mL PI solution. After that, cells were incubated with PI for 15 min at 37 °C in the dark to measure PI uptake following treatment. Fluorescence was measured in a fluorimeter (Fluorolog-3, HORIBA, USA) at an emission wavelength of 570–700 nm (2 nm slit width) and an excitation wavelength of 495 nm. The samples in the solution treated with DW were used as the negative control. Three independent tests were conducted on each condition.

2.8. Preparation of metabolites

The extraction of metabolites was done according to Wu, Zhao, Lai, and Yang (2021) with slight modifications. In order to get enough of the metabolites in bacterial cells, 600 g of fish fillets were used for each treatment. The inoculated and treated fish fillets were fully homogenised and then centrifuged twice (1400*g*, 2 min, 4 °C) to precipitate the fish debris ultimately. The supernatant was collected and centrifuged (12,000*g*, 10 min, 4 °C) to obtain *Aeromonas* cells. Resuspended cells with the pipette and then centrifuged to precipitate fragments at a low speed (2000*g*, 5 min, 4 °C). After centrifugation (12,000*g*, 15 min, 4 °C) and twice-washed with PBS, the mixture was suspended in a 5 mL extract solution (NaH_2PO_4-K_2HPO_4 buffer and acetonitrile 1:1 combination). Then, the sample was submerged in ice and subjected to a 25-cycle ultrasonic treatment (5 s ultrasonication followed by a 10 s break). The lysis cells were centrifuged (12,000*g*, 15 min, 4 °C) to collect metabolites, and the supernatant was transferred to a clean test tube. After that, added 5 mL extract to the pelletising residue, and the mixture was vortexed and centrifuged (12,000*g*, 15 min, 4 °C) to get the secondary supernatant. Samples were kept at 4 °C before usage. Each sample should be dissolved in 800 μL deuterated water containing 0.01 % TSP, centrifuged at 12,000*g* for 15 min at 4 °C, and transferred 600 μL supernatant to a 5 mm NMR tube.

2.9. NMR spectroscopic analysis

According to Zhao, Wu, Chen, and Yang (2019c), NMR spectra were produced with minor modifications. NMR studies at 298 K were performed using an NMR spectrometer and a triple inverse gradient probe (Brock, Germany). All samples were collected using a typical Bruker NOESY pulse train. Weak continuous wave irradiation was used to determine the water inhibition of cyclic delay (RD, 2 s) and mixing time (TM, 100 ms). Sixty-four transient signals with a spectral width of 20 ppm and a collection period of 1.36 s were recorded, totalling 32 K of data. All free induction attenuation was converted using an exponential window function with a 1 Hz widening factor before the Fourier transform. A 2D ^{1}H–^{13}C heterokaryotic single quantum coherent spectrum of one *Aeromonas* sample was acquired at 298 K using the Bruker hsqcedetgpsisp2.3 pulse sequence to identify metabolites. In the F2 and F1 channels, the ^{1}H spectra with a width of 10 ppm and the ^{13}C spectrum with a breadth of 180 ppm were examined, respectively (Chen et al., 2019).

2.10. Spectral analysis

The baseline, stage, and TSP signals were calibrated manually using TopSpin 4.1.3 software (Bruker Biospin, Rheinstetten, Germany). Non-overlapping signals from metabolites and an internal reference ratio (TSP) were integrated with TopSpin software, with metabolite integration equal to TSP integration to calculate metabolite concentrations to conduct quantitative analysis. The metabolites were identified collaboratively using peaks on ^{13}C and ^{1}H spectra using the Human Metabolome Database (https://wwww.hmdb.can) and relevant metabolomic studies (Chen et al., 2019, Chen et al., 2020, Lou et al., 2021). Mnova software was used to normalise peak values between 0.5 and 9.5 ppm (Mestreab, Research SL, Santiago de Compostela, Spain). The regional buckets were subdivided into 0.02 ppm increments, and container data was gathered for further processing.

SIMCA software was used for multivariate analysis (Version 13.0, Umetrics, Umea, Sweden). Separating groups and identifying related substances were accomplished using PCA and OPLS-DA. MetaboAnalyst 5.0 (https://www.metaboanalyst.ca/) and The Kyoto Encyclopedia of Genes and Genomes (KEGG) database(https://www.genome.jp/kegg/pathway.html) are used cooperatively to analyse and interpret the data.

2.11. Statistical analysis

Each experiment included at least three independent replications, and three parallel experimental groups were established. Microbiological analysis findings were converted to log CFU/g counts of barramundi. SPSS software (version 23, IBM Corp., Armonk, New York, USA) was used to perform the least significant difference (LSD) and analysis of variance (ANOVA). P-value < 0.05 was deemed statistically significant.

3. Results and discussion

3.1. Morphological features and strain identification

The morphological characteristics of single colonies are shown in Fig. S1. Colonies discovered in general were transparent, white to yellowish. Colonies were small in size and had a circular shape. The surface of the colony was raised or convex. Gram-negative rod-shaped cell morphology was detected under microscope. According to Culyba

and Van Tyne (2021), While genetic variations remind us of evolutionary links of bacteria, physical and biochemical traits remain critical for identifying and categorising these organisms. Indeed, bacteria are classed based on a variety of characteristics. Therefore, it is essential to consider the morphology of cells, the type of multicellular aggregation, motility, spore production, and gram staining. These morphological properties of bacteria, such as their form and colour, are not constant and may be altered by environmental factors. According to Batra, Mathur and Misra (2016) the *Aeromonas* spp. colony surface is rounded, raised, and smooth throughout. The colour of single colonies is transparent, ranging from white to light yellow. When seen under a microscope, they are Gram-negative rod-shaped bacteria. Therefore, according to the morphological features, it was reasonable to preliminarily speculate that the bacteria in the above samples were *Aeromonas*-like bacteria.

The assembly findings based on the DNA sequences of bacterium samples and the top 10 hits acquired from the NCBI database are displayed in Table S1. The top 10 hits derived from the phylogenetic tree are shown in Fig. 1. The results showed that all samples were *Aeromonas* isolates. The sample 3 and sample 4 were the same *Aeromonas* bacteria. As mentioned before, this may be because morphological properties of bacteria can be altered by environmental factors. The use of 16S rRNA gene sequences to research bacterial phylogeny and taxonomy has been one of the most often utilised housekeeping genetic markers (Manjul, & Shirkot, 2018). Thus, molecular analyses corroborated the morphological traits of the phylogenetic stage and established that the bacteria in these samples were *Aeromonas* spp.

3.2. Survival population of Aeromonas spp. after treatments and population changes during six days of cryopreservation

The antimicrobial activity of three *Aeromonas* strains under DW, CA, EW, and combined treatments was determined by enumerating bacterial colonies on LB agar. The survival population of three *Aeromonas* species under different treatments is shown in Fig. 2 (A-C). The initial number of *Aeromonas* strains inoculated on fish fillets was about 6 log CFU/g. After 5 min of treatment, the combined EW and CA treatment showed the best antibacterial performance, reducing the number of strain 1, strain 2, and strain 3 by 1.64, 1.69, and 1.66 log CFU/g, respectively. Combined treatment was more effective against strains 2 and 3 than strain 1. The three *Aeromonas* strains showed a significant difference in bactericidal effect between the DW, CA, EW, and the combined treatment group ($P < 0.05$). In addition, the effectiveness of these three sanitisation methods in descending order was CA + EW > CA > EW. Some researchers also obtained similar results and found that the bactericidal effect of the combined treatment group was better than that of the individual treatment group, when EW and organic acids are used together, the number of bacteria in different foods was significantly reduced (Tango et al., 2015, Zhao, Zhao, Phey, & Yang, 2019).

The growth curve of three *Aeromonas* strains on fish fillets under different treatments during cold storage is shown in Fig. 3 (A-C). All strains showed specific growth curves in both fish models, similar to the growth curves of bacteria observed by Lou et al. (2021) in the early stage of cryopreservation in the fish decay model. Compared with the other treatment groups, the number of bacteria in the control group entered the stable stage more quickly. Taking 7 log CFU/g as the reference line for the number of bacteria, it can be found that the time for the three bacteria to reach the concentration standard under different treatment methods is in the order of CA + EW > CA > EW > DW. On the other hand, it proved that the combined treatment group had higher antibacterial ability against the three *Aeromonas* species. Another study also reported comparable results, and they found that the combined treatment of CA and EW rapidly reduced the total bacterial count in carrot shreds, improved the freshness and cleanliness of carrots, and extended their refrigeration time (Rahman et al., 2011).

3.3. Cell membrane integrity analysis

PI is a DNA-embedded fluorescent probe that can penetrate bacteria with broken cell membranes and fluorescein when it binds to nucleic acids (Rosenberg, Azevedo, & Ivask, 2019). Therefore, the PI uptake assay can determine the extent of cell membrane damage produced by CA and/or EW in three *Aeromonas* species. The fluorescence spectrum of the PI-bacterial mixture (Fig. 4) revealed that the DW sample had a considerably lower PI influx than the other three treatments, showing that both CA and EW might cause cell membrane breakdown and impair cell membrane integrity. Additionally, using 630 nm wavelength as the reference line, the degree of damage to the bacterial cell membrane

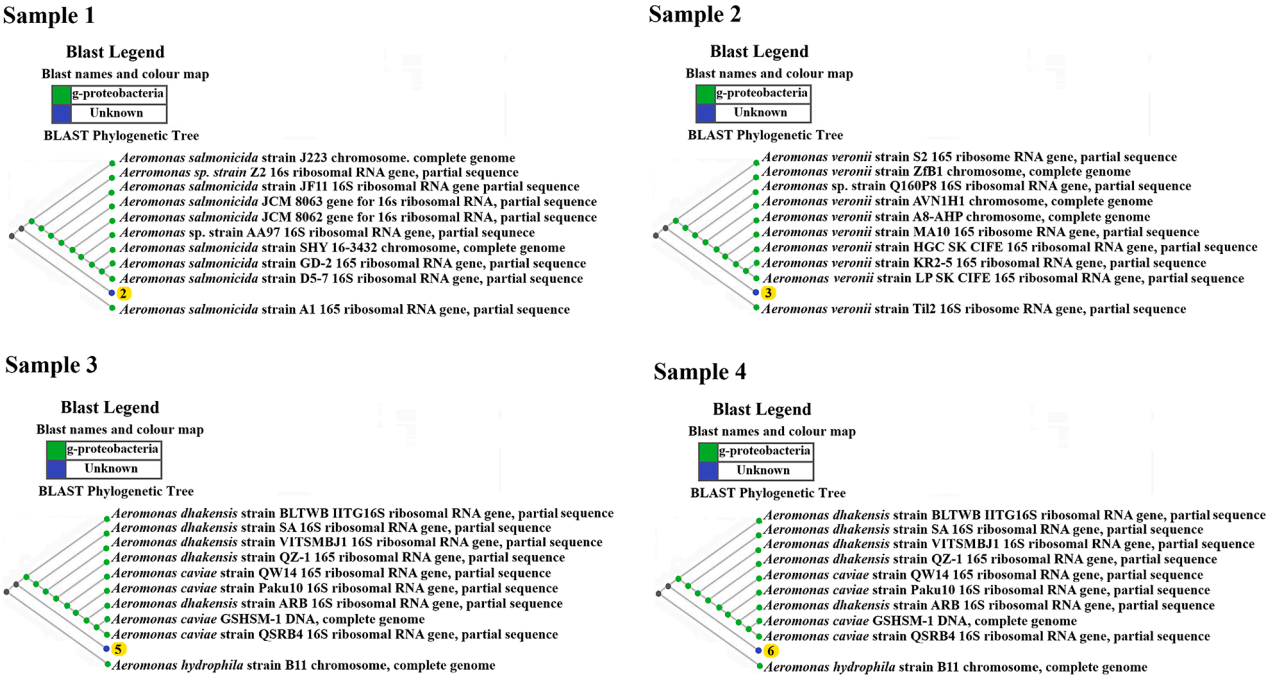

Fig. 1. The phylogenetic tree analysis of samples – neighbour-joining by NCBI blast tree method.

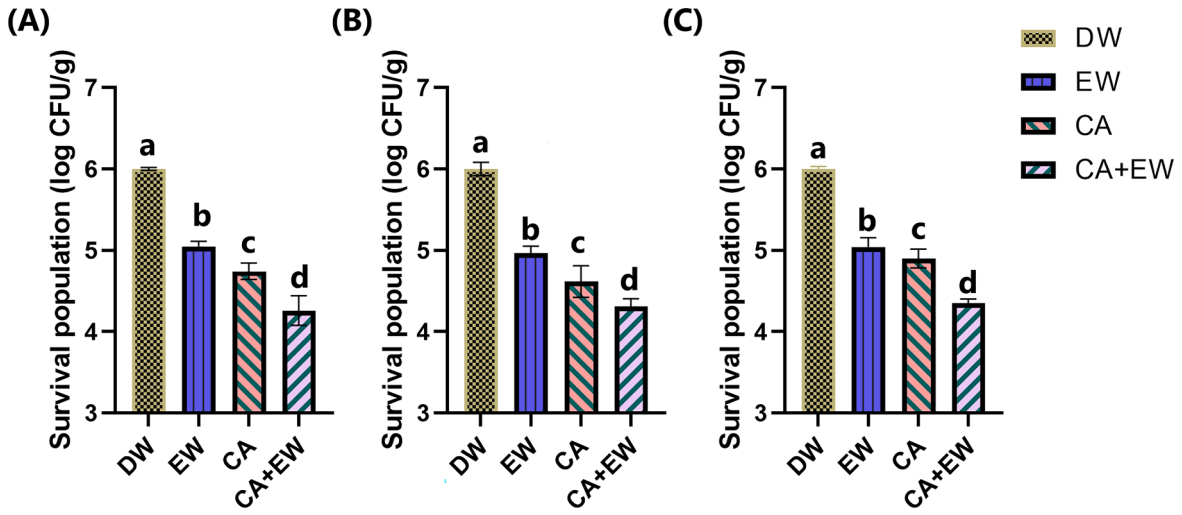

Fig. 2. The survival populations of strain 1 (A), strain 2 (B), and strain 3 (C) under treatments. Notes: deionised water (DW), citric acid (CA), electrolysed water (EW), and 1 % citric acid + electrolysed water (CA + EW); a-d: different letters mean significant differences among different samples with the same media ($P < 0.05$).

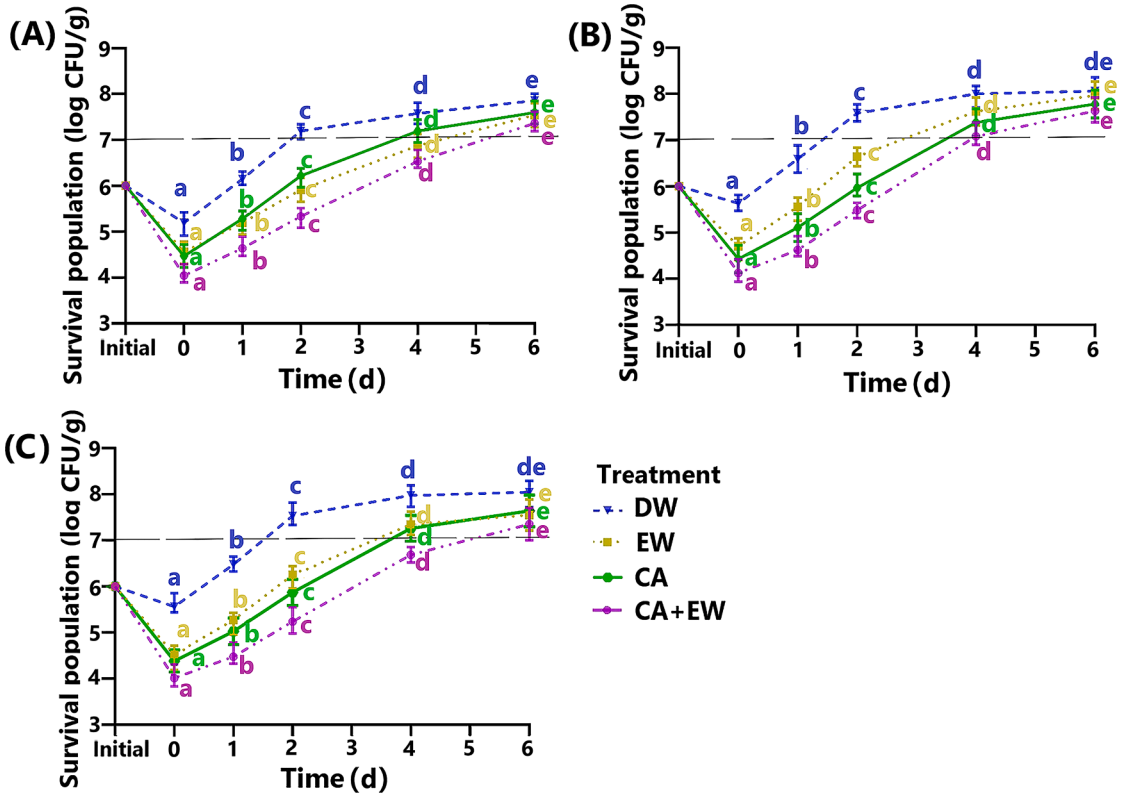

Fig.3. Population changes of fish fillets inoculated with strain 1 (A), strain 2 (B), and strain 3 (C) during storage under different treatments. Notes: deionised water (DW), citric acid (CA), electrolysed water (EW), and 1 % citric acid + electrolysed water (CA + EW); a-e: different letters mean the significant difference among different samples ($P < 0.05$).

caused by the four treatments was CA + EW > CA > EW > DW, demonstrating that the combination of CA and EW increased the detrimental effects on cell membrane integrity. The synergistic loss of cell membrane integrity by CA and EW may be due to their particular action sites and modes on the bacterial cell membrane, allowing CA and EW to assault the cell membrane in numerous dimensions. Weak organic acids also inhibit microbial growth through membrane disruption caused by proton dynamics, membrane transport, and stress responses to intracellular pH homeostasis, resulting in increased energy expenditure and suppression of fundamental metabolic processes (McDermott et al., 2018). Furthermore, significant chlorine compounds in EW, such as HClO and $^{-}$OCl, may compromise membrane integrity (Hati et al., 2012). These studies corroborate our findings, indicating that CA and EW have antibacterial activity against the cell membrane.

3.4. *Metabolic profiles of Aeromonas strains*

The metabolic profiles of *Aeromonas* bacteria inoculated on barramundi after different treatments during cold storage are shown in Fig S2. Metabolites with ^{1}H and ^{13}C chemical shifts as peak distributions are

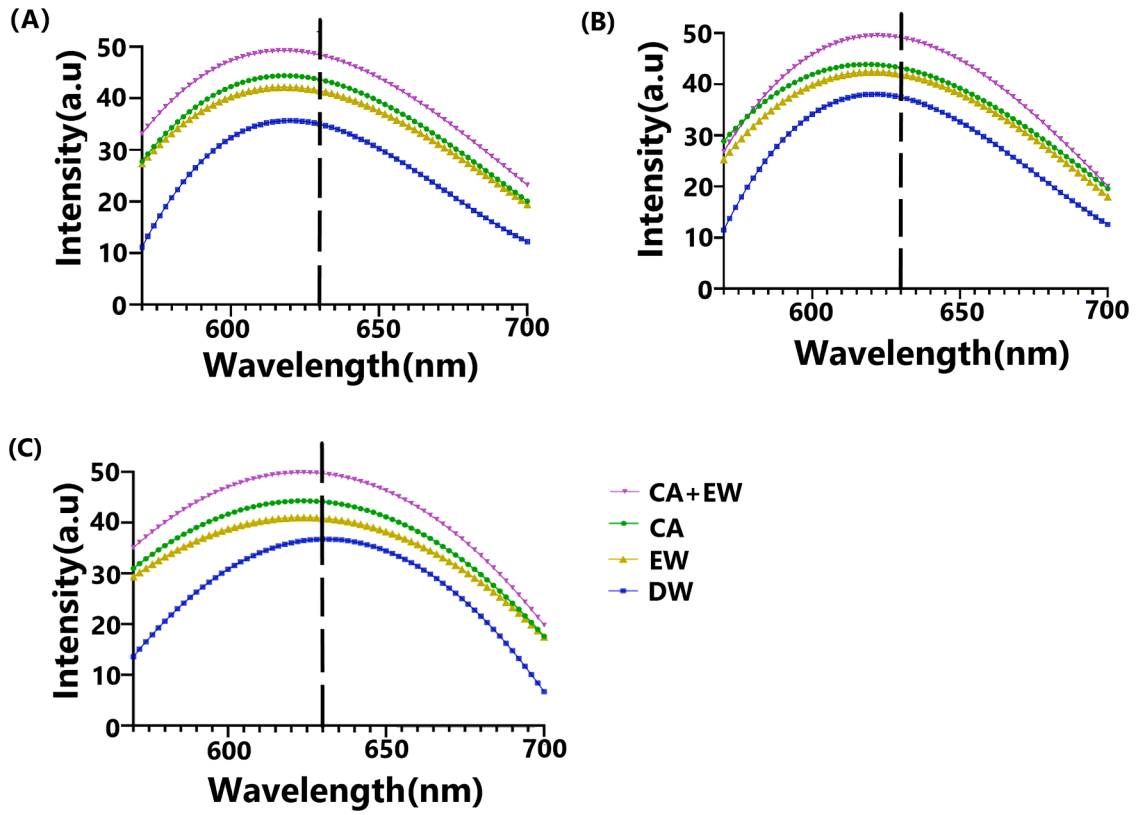

Fig.4. The fluorescence spectra of propidium iodide in three *Aeromonas* strains treated with deionised water (DW), citric acid (CA), electrolysed water (EW), and 1 % citric acid + electrolysed water (CA + EW) for 6 h. Note: A: strain 1, B: strain 2, C: strain 3.

shown in Table S2. Multiple signals from 1.0 to 9.0 ppm were recorded and detected over a six-day storage period. Most signals were in the range of 1.0 – 5.0 ppm for all groups. The intensity of most ^{1}H signals in the range 7.0 – 9.0 ppm changed significantly with prolonged storage time, suggesting that some metabolites were formed during cold storage while others were degraded.

According to the chemical shift of ^{1}H NMR and 2D ^{1}H–^{13}C NMR spectra, a total of 36 metabolites were determined, and 35 of them were quantified. The metabolome of the three *Aeromonas* species comprises 13 amino acids, 1 dipeptide, 5 organic acids, 2 carbohydrates, 1 alcohol, 5 bioamines, 6 nucleotides, and 3 other components. NMR spectra showed three definite regions. The first region was between 0.5 and 3.0 ppm, primarily amino acids [e.g., Leucine (Leu), isoleucine (Ile), valine (Val)] and certain organic acids (e.g., lactic acid, acetic acid) were discovered. The second region was between 3.0 and 5.5 ppm, and primary carbohydrates (e.g., α-glucose and β-glucose) were discovered. The last region was between 5.5 and 9.0 ppm, and primary adenosine triphosphate (ATP) breakdown products [e.g., adenosine monophosphate (AMP), inosine monophosphate (IMP)] were discovered. (Shumilina, Ciampa, Capozzi, Rustad, & Dikiy, 2015, Marchetti, Pellati, Benvenuti, & Bertelli, 2019).

3.5. Alternative metabolites during the individual treatment of CA and/or EW during storage

To better understand the metabolic alterations caused by each treatment, measured a total of 35 metabolites with distinctive chemical peaks in the heat map. The concentration of the metabolite following log10 transformation is shown in Fig S3. The deeper greens and reds on the heat map represent metabolite concentrations that are lower and greater, respectively. It is interesting to note that although the observed metabolites in different strains have a certain difference, compared with the control group, after CA and/or EW treatment, three *Aeromonas* strains detected metabolites of accumulation and consumption trend basically the same. This finding showed that although three *Aeromonas* strains were different, they showed high similarity in response to CA and/or EW stress. Our findings corroborate prior assessments of metabolite concentrations in *A. Salmonicid*a, and biogenic amines exhibit substantial variation in identified metabolites (Jakobsen, Shumilina, Lied, & Hoel, 2020). Both EW and CA treatment inhibited *Aeromonas* spp. from producing significant metabolites such as alcohols (2, 3-Butanediol), some amino acids [e.g., Ile, Leu, Val, Ala (alanine)], and ammonia (putrescine). The decrease of ATP level and the increase of Glu level indicated that the combined treatment resulted in the decrease of the glucose utilisation rate of the three strains and inhibited the energy supplement of the metabolic pathway. The hypothesised method is shown in Fig. 5.

In CA, the antimicrobial effect occurs by reducing the pH of a medium or food to prevent microbial growth. Organic acid molecules that are not dissociated and uncharged are initially responsible for antibacterial action since their concentration rises at low pH (Bushell, Tonner, Jabbari, Schmid, & Lund, 2019). Due to the lipophilicity of these undissociated molecules, they are thought to easily pass through the lipid membranes of target microorganisms and into their cytoplasm, resulting in cell death (McDermott et al., 2018). Indeed, once within the cytoplasm of a bacterial or fungal cell, organic acid molecules are exposed to elevated pH levels and break down into negatively charged anions and protons that cannot pass through the plasma membrane (Lund et al., 2020). Accumulated H^{+} ions lower the intracellular pH, causing cell damage and functional alterations in enzymes, structural proteins, and DNA (Stratford et al., 2013). Additionally, the anions created have been demonstrated to be hazardous, inhibiting metabolic pathways and resulting in cell death (Anyasi et al., 2017). On the other hand, releasing these anions raises cytoplasmic osmotic pressure, which is detrimental to cell solute enzymes (Wood, 2015).

In EW, oxidising chemicals found in EW, including hydrogen

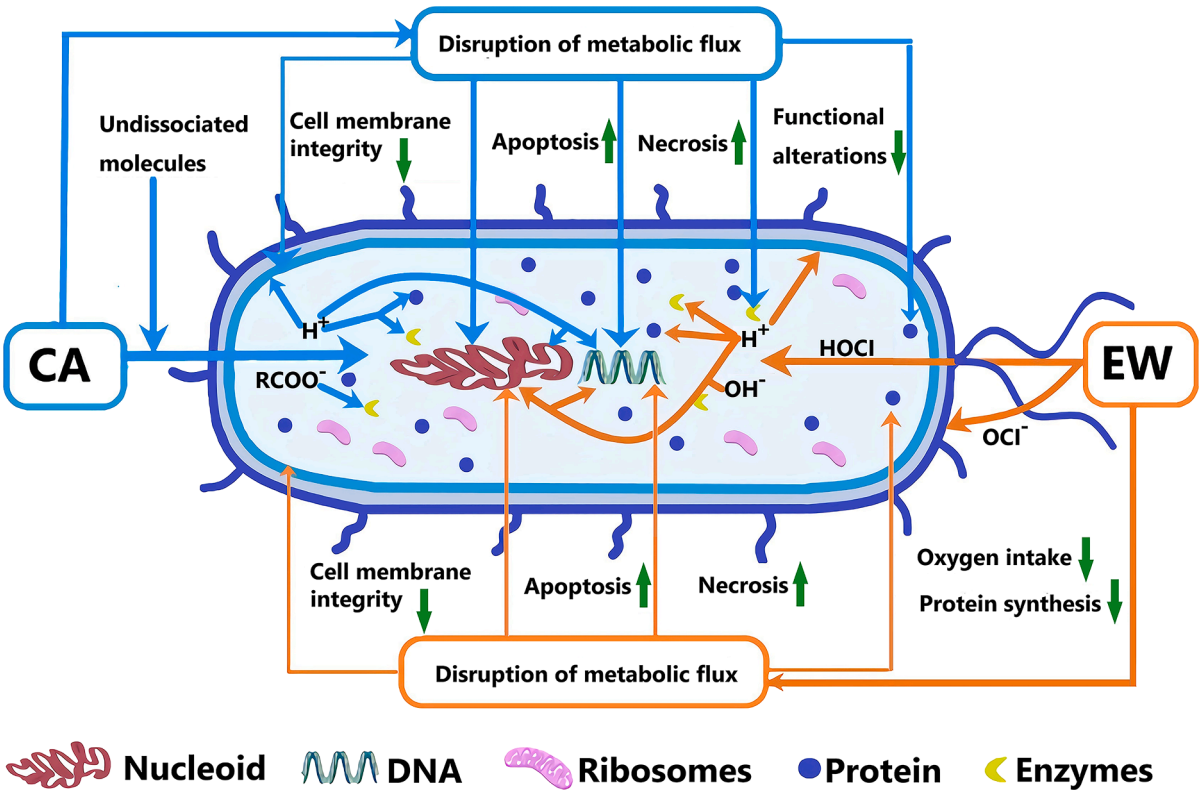

Fig. 5. The citric acid (CA) and electrolysed water (EW) bactericidal actions proposed principles. The antibacterial mechanism of EW and CA are shown in orange and blue boxes, respectively. (For interpretation of the references to colour in this figure legend, the reader is referred to the web version of this article.)

peroxide (H_2O_2) and superoxide anion (O^2), may disrupt the redox state of cells, resulting in pathogen necrosis and apoptosis (Schieber & Chandel, 2014). Additionally, significant chlorine molecules, such as HClO and $^{\cdot}$OCl, may alter metabolic flux and protein synthesis, damage membrane integrity, infiltrate cells, impede glucose oxidation, and decrease oxygen intake (Hati et al., 2012). In general, reactive cells, such as amino acids and peptide bonds, are susceptible to EW, resulting in adverse metabolic responses and metabolite alterations (Zhao, Zhao, Wu, Lou, & Yang, 2019b).

3.6. Metabolite quantification analysis of combined treatment

The amounts of metabolites produced by *Aeromonas* spp. were determined, as indicated in Table 1 (A-C). While the metabolites of glycine (Gly), taurine (Tau), lactic acid, creatine, glucose, trimethylamine-N-oxide (TMAO), ATP, AMP, adenosine, IMP, choline, and glycolic acid decreased throughout the six-day storage period, the other metabolites increased significantly ($P < 0.05$). Acetic acid was increased 6.5 to 8.0-fold, hypoxanthine was increased 5.7 to 7.7-fold, inosine was increased 4.0–4.3-fold, and dimethylamine (DMA) was increased 1.6 to 2.6-fold. Most amino acids rose in concentration by around one to thrice. By comparison, the quantity of Gly, adenosine, lactic acid, and IMP was dramatically reduced. The growing and decreasing metabolites of *Aeromonas* under the combination treatment followed the same pattern as the DW treatment, but the change rate and total amount were relatively low. Acetic acid increased 6.2 to 7.4-fold, hypoxanthine was increased 5.5 to 6.9-fold, inosine was increased 3.6 to 3.7-fold, and dimethylamine was increased 1.2 to 1.8-fold, with varying degrees of reduction. It can be found that the combined treatment significantly reduced the rate of metabolite change in the six-day storage experiment compared with the DW group ($P < 0.05$) by comparing the content of metabolites. This can also reflect that the combined treatment has an excellent antibacterial effect on *Aeromonas* spp.

The change in metabolite content could be due to the combined treatment interfering with the normal metabolism of the bacteria. The spoilage bacteria multiply fast and create many proteolytic enzymes during the preliminary stages of fish corruption (Yoshioka, Konno, & Konno, 2019). The decrease of intracellular TMAO content and the increase of trimethylamine (TMA) content indicated that it could reduce TMAO to TMA during the spoilage of barramundi. This is like the results obtained by other researchers in which *A. Salmonicida* isolated from common carp produced a slight odour characterised by “cheese and acid” and TMAO to TMA (Beaz-Hidalgo et al., 2015). In addition, it has been reported that the concentration of TMA in frozen raw salmon samples inoculated with *A. Salmonicida* was significantly higher than that in uninoculated samples (Jakobsen et al., 2020). The decomposition of protease can produce amino acids. The increase in the amino acid concentration of the three *Aeromonas* strains proved that the three strains had protease activity. Another study also reported comparable results, which discovered that *Aeromonas* isolates linked with fish and meat deterioration were classified as slime makers, with 95 % of isolates exhibiting lipase and protease activity (Arslan & Küçüksari, 2015).

3.7. Comparison of metabolites in Aeromonas strains during storage under combined treatment

PCA was used to examine the differences between metabolites and group identification to understand better the variations between the three *Aeromonas* strains after six days of storage. The model’s quality, grouping information, metabolites, R^2X and Q^2 scores are depicted in Fig. 6.

PC1 and PC2 together accounted for 79.9 % of the entire dataset (PC1: 63.8 %; PC2: 16.1 %), and the model’s Q^2 score (0.782 > 0.50) indicates that it is highly predictive. In the score plot, the samples of each *Aeromonas* strain under different treatments on the same day were separated but gathered under the same treatment. In addition, the samples of each *Aeromonas* strain on different days under the same

Table 1
Metabolite contents produced by three strains of *Aeromonas* spp. during 6 °C storage.

Table A	Mean content (mM)					
	DW			CA + EW		
Metabolites	DAY0	DAY4	DAY6	DAY0	DAY4	DAY6
Leu	0.153^{a}	0.243^{b}	0.415^{c}	0.147^{d}	0.217^{e}	0.373^{f}
Ile	0.495^{a}	0.907^{b}	1.310^{c}	0.271^{d}	0.555^{e}	0.848^{f}
Val	0.083^{a}	0.118^{b}	0.173^{c}	0.073^{d}	0.100^{e}	0.118^{ef}
Met	0.046^{a}	0.079^{b}	0.138^{c}	0.045^{d}	0.065^{de}	0.090^{ef}
Lys	0.108^{a}	0.215^{b}	0.248^{c}	0.033^{d}	0.176^{e}	0.197^{ef}
Phe	0.083^{a}	0.110^{b}	0.138^{c}	0.073^{d}	0.098^{e}	0.116^{f}
Ala	0.685^{a}	1.395^{b}	2.132^{c}	0.599^{d}	1.157^{e}	1.651^{f}
Tyr	0.049^{a}	0.225^{b}	0.178^{c}	0.039^{d}	0.150^{e}	0.164^{ef}
Gly	4.966^{a}	3.688^{b}	2.461^{c}	4.649^{d}	3.343^{e}	2.133^{f}
Tau	2.059^{a}	1.855^{b}	1.755^{c}	2.229^{d}	2.178^{e}	2.113^{f}
Gln	0.241^{a}	0.745^{b}	0.840^{c}	0.233^{d}	0.478^{e}	0.575^{f}
Glu	0.243^{a}	0.358^{b}	0.490^{c}	0.201^{d}	0.288^{e}	0.343^{f}
Arg	0.205^{a}	0.374^{b}	0.465^{c}	0.145^{d}	0.280^{e}	0.363^{f}
Anserine	0.097^{a}	0.188^{b}	0.205^{bc}	0.077^{d}	0.128^{e}	0.148^{ef}
Lactic acid	4.805^{a}	3.092^{b}	2.205^{c}	4.704^{d}	2.332^{e}	1.523^{f}
Acetic acid	0.093^{a}	0.530^{b}	0.744^{c}	0.085^{d}	0.460^{e}	0.610^{f}
Succinic acid	0.140^{a}	0.413^{b}	0.548^{c}	0.095^{d}	0.250^{e}	0.398^{f}
Creatine	7.641^{a}	5.859^{b}	4.711^{c}	8.408^{d}	7.158^{e}	6.014^{f}
Glucose	0.015^{a}	0.012^{ab}	0.009^{abc}	0.017^{d}	0.015^{de}	0.013^{def}
2,3-butanediol	0.045^{a}	0.053^{ab}	0.055^{abc}	0.040^{d}	0.040^{de}	0.044^{def}
TMAO	7.117^{a}	5.953^{b}	5.559^{c}	7.577^{d}	6.786^{e}	6.399^{f}
TMA	0.125^{a}	0.199^{b}	0.277^{c}	0.118^{d}	0.165^{e}	0.198^{f}
DMA	0.010^{a}	0.014^{ab}	0.018^{abc}	0.010^{d}	0.011^{de}	0.012^{def}
Tyramine	0.030^{a}	0.204^{b}	0.229^{c}	0.030^{d}	0.115^{e}	0.183^{f}
ATP	0.018^{a}	0.015^{bc}	0.013^{abc}	0.017^{c}	0.014^{de}	0.010^{f}
AMP	0.250^{a}	0.148^{b}	0.128^{bc}	0.242^{d}	0.108^{e}	0.061^{f}
Adenosine	0.203^{a}	0.173^{b}	0.138^{c}	0.201^{d}	0.145^{e}	0.093^{f}
IMP	0.143^{a}	0.125^{b}	0.101^{c}	0.133^{d}	0.121^{e}	0.092^{f}
Inosine	0.068^{a}	0.140^{b}	0.280^{c}	0.066^{d}	0.138^{e}	0.246^{f}
Hypoxanthine	0.066^{a}	0.296^{b}	0.421^{c}	0.059^{d}	0.266^{e}	0.358^{f}
Betaine	0.733^{a}	1.221^{b}	1.730^{c}	0.523^{d}	0.922^{e}	1.206^{f}
Choline	0.064^{a}	0.055^{ab}	0.028^{c}	0.058^{d}	0.045^{de}	0.022^{ef}
Creatinine	0.198^{a}	0.220^{b}	0.243^{c}	0.195^{d}	0.208^{de}	0.220^{ef}
glycolic acid	5.533^{a}	4.783^{b}	3.767^{c}	6.003^{d}	5.439^{e}	4.683^{f}
Putrescine	0.682^{a}	1.760^{b}	2.674^{c}	0.475^{d}	1.530^{e}	2.355^{f}
Table B	**Mean content (mM)**					
	DW			CA+EW		
Metabolites	DAY0	DAY4	DAY6	DAY0	DAY4	DAY6
Leu	0.212^{a}	0.253^{b}	0.412^{c}	0.211^{d}	0.227^{de}	0.394^{f}
Ile	0.437^{a}	0.784^{b}	1.437^{c}	0.247^{d}	0.543^{e}	0.801^{f}
Val	0.129^{ab}	0.148^{ab}	0.229^{c}	0.080^{d}	0.113^{e}	0.150^{f}
Met	0.051^{a}	0.086^{b}	0.149^{c}	0.047^{de}	0.077^{e}	0.097^{f}
Lys	0.110^{a}	0.150^{b}	0.180^{c}	0.043^{d}	0.126^{e}	0.163^{f}
Phe	0.129^{a}	0.155^{b}	0.189^{c}	0.100^{d}	0.123^{e}	0.167^{f}
Ala	0.952^{a}	1.370^{b}	1.952^{c}	0.657^{d}	1.203^{e}	1.470^{f}
Tyr	0.093^{a}	0.178^{b}	0.293^{c}	0.047^{d}	0.121^{e}	0.213^{f}
Gly	5.980^{a}	4.733^{b}	3.980^{c}	5.339^{d}	4.100^{e}	3.254^{f}
Tau	2.820^{a}	2.610^{b}	2.520^{c}	3.058^{d}	2.944^{e}	2.878^{f}
Gln	0.187^{a}	0.229^{b}	0.287^{c}	0.113^{d}	0.207^{e}	0.278^{f}
Glu	0.246^{a}	0.298^{b}	0.396^{c}	0.207^{d}	0.270^{e}	0.320^{f}
Arg	0.257^{a}	0.432^{b}	0.557^{c}	0.170^{d}	0.347^{e}	0.470^{f}
Anserine	0.196^{a}	0.247^{b}	0.296^{c}	0.126^{d}	0.166^{e}	0.182^{ef}
Lactic acid	5.463^{a}	3.726^{b}	3.030^{c}	5.254^{d}	3.106^{e}	2.454^{f}
Acetic acid	0.090^{a}	0.370^{b}	0.590^{c}	0.086^{d}	0.313^{e}	0.529^{f}
Succinic acid	0.203^{a}	0.403^{b}	0.603^{c}	0.143^{d}	0.358^{e}	0.507^{f}
Creatine	7.658^{a}	6.168^{b}	5.258^{c}	8.524^{d}	7.646^{e}	6.450^{f}
Glucose	0.027^{a}	0.020^{ab}	0.017^{abc}	0.028^{d}	0.023^{de}	0.020^{def}
2,3-butanediol	0.060^{a}	0.061^{ab}	0.063^{abc}	0.058^{d}	0.059^{de}	0.061^{def}
TMAO	7.725^{a}	6.182^{b}	5.825^{c}	8.169^{d}	6.892^{e}	6.294^{f}
TMA	0.173^{a}	0.226^{b}	0.293^{c}	0.167^{d}	0.213^{e}	0.247^{f}
DMA	0.013^{a}	0.019^{ab}	0.034^{bc}	0.013^{a}	0.014^{ab}	0.024^{abc}
Tyramine	0.042^{a}	0.208^{b}	0.242^{c}	0.043^{d}	0.141^{e}	0.220^{f}
ATP	0.023^{a}	0.017^{ab}	0.013^{ec}	0.020^{d}	0.015^{de}	0.012^{def}
AMP	0.322^{a}	0.237^{b}	0.107^{c}	0.227^{d}	0.110^{e}	0.067^{ef}
Adenosine	0.280^{a}	0.253^{b}	0.193^{c}	0.203^{d}	0.137^{e}	0.081^{f}
IMP	0.154^{a}	0.144^{ab}	0.126^{c}	0.151^{d}	0.139^{de}	0.111^{f}
Inosine	0.070^{a}	0.132^{b}	0.281^{c}	0.068^{d}	0.128^{e}	0.248^{f}
Hypoxanthine	0.067^{a}	0.274^{b}	0.381^{c}	0.066^{d}	0.258^{e}	0.366^{f}
Betaine	0.954^{a}	1.296^{b}	1.544^{c}	0.792^{d}	1.117^{e}	1.337^{f}

(*continued on next page*)

Table 1 (*continued*)

Table B	Mean content (mM)					
	DW			CA+EW		
Metabolites	**DAY0**	**DAY4**	**DAY6**	**DAY0**	**DAY4**	**DAY6**
Choline	0.106^{a}	0.080^{b}	0.056^{c}	0.103^{d}	0.072^{de}	0.046^{f}
Creatinine	0.229^{a}	0.250^{b}	0.289^{c}	0.225^{d}	0.242^{e}	0.273^{f}
glycolic acid	5.832^{a}	5.167^{b}	4.132^{c}	6.435^{d}	5.966^{e}	5.143^{f}
Putrescine	0.669^{a}	1.839^{b}	2.669^{c}	0.452^{d}	1.402^{e}	2.387^{f}
Table C	**Mean content (mM)**					
	DW			**CA+EW**		
Metabolites	**DAY0**	**DAY4**	**DAY6**	**DAY0**	**DAY4**	**DAY6**
Leu	0.206^{a}	0.298^{b}	0.406^{c}	0.205^{d}	0.221^{de}	0.336^{f}
Ile	0.403^{a}	0.809^{b}	1.403^{c}	0.268^{d}	0.514^{e}	0.603^{f}
Val	0.114^{a}	0.127^{b}	0.200^{c}	0.109^{d}	0.119^{de}	0.182^{f}
Met	0.041^{a}	0.087^{b}	0.131^{c}	0.035^{d}	0.069^{e}	0.098^{f}
Lys	0.034^{a}	0.129^{b}	0.154^{c}	0.032^{d}	0.122^{e}	0.133^{ef}
Phe	0.100^{a}	0.143^{b}	0.188^{c}	0.097^{d}	0.129^{e}	0.158^{f}
Ala	0.934^{a}	1.260^{b}	1.934^{c}	0.688^{d}	0.870^{e}	1.200^{f}
Tyr	0.082^{a}	0.208^{b}	0.282^{c}	0.069^{d}	0.122^{e}	0.167^{f}
Gly	4.923^{a}	3.253^{b}	1.923^{c}	4.245^{d}	2.601^{e}	1.313^{f}
Tau	2.062^{a}	1.852^{b}	1.662^{c}	2.937^{d}	2.790^{e}	2.678^{f}
Gln	0.198^{a}	0.246^{b}	0.298^{c}	0.182^{d}	0.220^{e}	0.233^{ef}
Glu	0.125^{a}	0.319^{b}	0.425^{c}	0.117^{d}	0.254^{e}	0.304^{f}
Arg	0.365^{a}	0.567^{b}	0.665^{c}	0.232^{d}	0.411^{e}	0.592^{f}
Anserine	0.102^{a}	0.189^{b}	0.202^{bc}	0.100^{d}	0.137^{e}	0.155^{f}
Lactic acid	5.037^{a}	3.460^{b}	2.784^{c}	5.010^{d}	2.601^{e}	2.004^{f}
Acetic acid	0.089^{a}	0.460^{b}	0.641^{c}	0.080^{d}	0.381^{e}	0.593^{f}
Succinic acid	0.401^{a}	0.541^{b}	0.601^{c}	0.383^{d}	0.436^{e}	0.573^{f}
Creatine	7.785^{a}	5.893^{b}	4.885^{c}	8.412^{d}	6.772^{e}	5.817^{f}
Glucose	0.061^{a}	0.015^{b}	0.011^{bc}	0.086^{d}	0.022^{e}	0.014^{ef}
2,3-butanediol	0.033^{a}	0.050^{b}	0.053^{c}	0.031^{d}	0.046^{de}	0.051^{def}
TMAO	7.527^{a}	5.739^{b}	5.527^{c}	7.957^{d}	6.758^{e}	6.190^{f}
TMA	0.146^{a}	0.206^{b}	0.236^{c}	0.139^{d}	0.154^{de}	0.191^{f}
DMA	0.016^{a}	0.022^{ab}	0.025^{abc}	0.014^{d}	0.014^{de}	0.017^{def}
Tyramine	0.062^{a}	0.217^{b}	0.262^{c}	0.053^{d}	0.198^{e}	0.244^{f}
ATP	0.025^{a}	0.018^{ab}	0.017^{abc}	0.023^{d}	0.016^{de}	0.014^{ef}
AMP	0.327^{a}	0.144^{b}	0.116^{c}	0.287^{d}	0.102^{e}	0.066^{f}
Adenosine	0.238^{a}	0.208^{b}	0.130^{dc}	0.228^{d}	0.144^{e}	0.088^{f}
IMP	0.163^{a}	0.140^{b}	0.129^{c}	0.161^{d}	0.125^{e}	0.108^{ef}
Inosine	0.058^{a}	0.117^{b}	0.248^{c}	0.055^{d}	0.092^{e}	0.205^{ef}
Hypoxanthine	0.063^{a}	0.341^{b}	0.486^{c}	0.059^{d}	0.282^{e}	0.410^{f}
Betaine	1.238^{a}	1.427^{b}	1.638^{c}	0.902^{d}	1.351^{e}	1.501^{f}
Choline	0.048^{a}	0.020^{b}	0.018^{bc}	0.038^{d}	0.016^{e}	0.012^{ef}
Creatinine	0.240^{a}	0.247^{ab}	0.270^{c}	0.218^{d}	0.223^{de}	0.258^{f}
glycolic acid	5.134^{a}	4.385^{b}	3.334^{c}	5.727^{d}	5.112^{e}	4.348^{f}
Putrescine	0.611^{a}	1.958^{b}	2.811^{c}	0.404^{d}	1.541^{e}	2.170^{f}

Notes: Table A: strain 1; Table B: strain 2; Table c: strain 3; deionised water (DW); 1 % citric acid + electrolysed water (CA + EW); a-c: Different letters mean the significant difference among different days in the deionised water group; d-f: Different letters mean the significant difference among different days in 1 % citric acid + electrolysed water group ($P < 0.05$).

treatment also showed apparent separation (Fig. 6B). For example, on day 0, under the DW treatment and CA + EW treatment, the three strains were all in the positive pole of PC1 and PC2, whereas day 4 was in the positive poles of PC1 and the negative poles of PC2. On day 6, strain 1 was situated in the negative poles of PC1 and PC2. However, strain 2 and strain 3 were both positioned in the negative poles of PC1 and PC2, in contrast to day 0. In addition, it can be shown that the three bacteria on the fish fillets treated with DW had a greater inclination toward the negative pole than those treated with CA + EW, indicating that the combined treatment group had an antibacterial effect.

OPLS-DA cross-validation score and coefficient coding loading plots based on day 6 were created to observe the metabolic changes in *Aeromonas* spp. under combined treatment in the barramundi model more intuitively. Based on R^2X and Q^2 values, all published OPLS-DA models demonstrated high predictability and interpretability. The pairwise comparison of OPLS-DA metabolites of three *Aeromonas* strains in sterile fish fillets under different conditions is shown in Fig S4. The load S-line is depicted in warm hues to indicate probable identifying metabolites. Significant metabolites were identified in this investigation as those having a VIP > 1, absolute correlation coefficient > 0.602 and $P < 0.05$. Each pair was separated on the score plot, indicating that the antibacterial action of the combined treatment was evident at the metabolic level. The S-line provides a clear view of compounds with metabolic differences. The downward peak implies that the combined treatment group has a lower metabolite concentration than the control group and vice versa. There were 13, 13, and 14 metabolites produced by strain 1 to strain 3 under different treatments that were significantly affected. Under combined treatment, the organic acid content of strains was dramatically decreased, and the concentration of 2, 3-butanediol dropped. Additionally, glucose, some nucleotide-related chemicals, and secondary metabolites such as putrescine, choline, and betaine were dramatically decreased, consistent with the dropping trend of dominating metabolites.

3.8. Pathway analysis

Pathway analysis was used to investigate the interaction of each strain's metabolic network under combined treatment stress. MetaboAnalyst 5.0 predicted all impacted pathways based on the substantially detected metabolites filtered out in section 3.6. During the metabolic

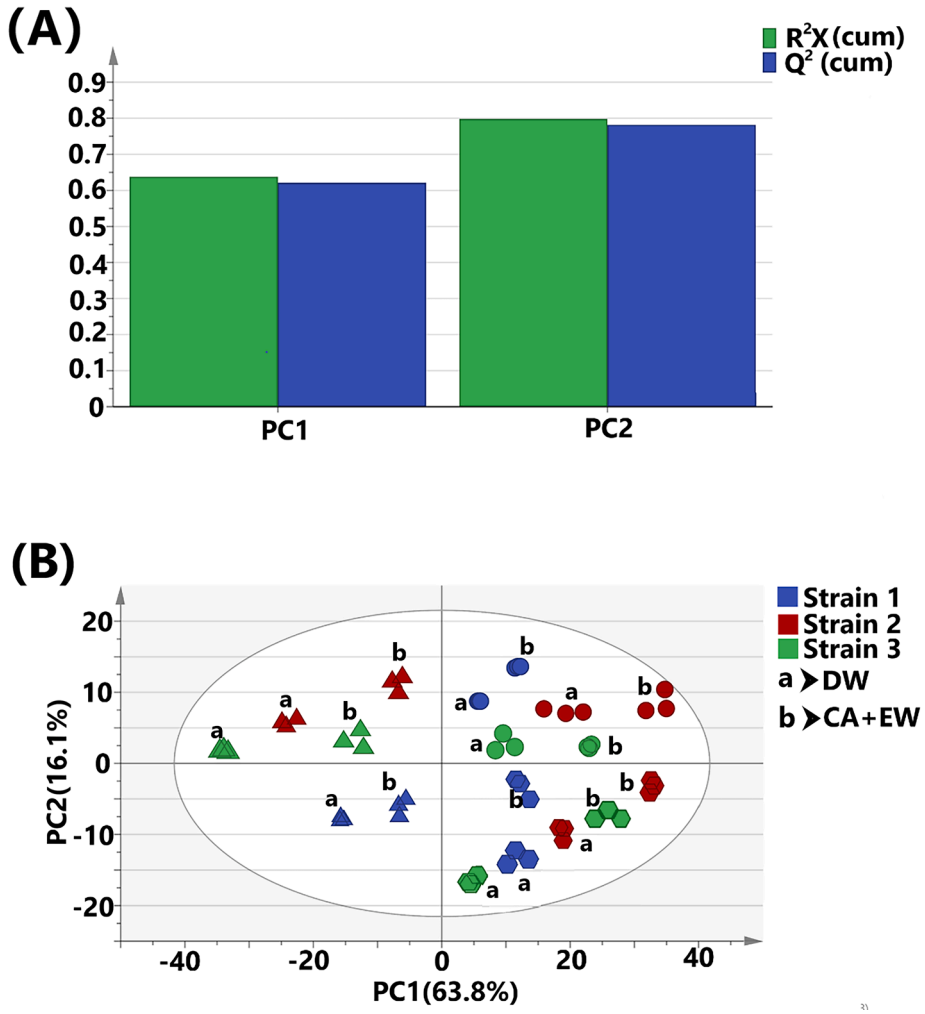

Fig. 6. Principal component analysis (PCA) of ^{1}H NMR spectra of three *Aeromonas* strains in control and combined groups for 6-day storage. Principal components explain the variances in PCA (A); the score plot of PCA (B). Note: round: day 0; hexagon: day 4; triangular: day 6; deionised water (DW); 1 % citric acid + electrolysed water (CA + EW).

process of the three bacteria strains, a total of 38 pathways were anticipated; 20, 31, and 31 pathways were significantly disrupted in strain 1, strain 2, and strain 3, respectively ($P < 0.05$). The disrupted pathways are primarily involved in amino acid, energy, and carbohydrate metabolism. The findings are summarised in Table S3, which is shown in Fig S5. The co-uptake of the three *Aeromonas* strains is mediated by 13 pathways, including aminoacyl-tRNA biosynthesis; Methane metabolism; D-glutamine and D-glutamate metabolism; Nitrogen metabolism; Pyruvate metabolism; Phenylalanine, tyrosine, and tryptophan biosynthesis; Glyoxylate and Dicarboxylate metabolism; Novobiocin biosynthesis; Glutathione metabolism; Glycine, Serine, and Threonine metabolism; Arginine and proline metabolism; Tyrosine metabolism; Phenylalanine metabolism. Seven more pathways have also been dramatically altered for strain 1. Sixteen more pathways were substantially changed in strain 2 and 3. The number of significantly changed pathways indicated that the combined treatment was more effective for strain 2 and strain 3 than strain 1, which was also confirmed in Section 3.2. The hypothetical schematic depicting metabolic alterations in all three strains in response to combined treatment exposure based on the KEGG database is shown in Fig. 7.

In general, the synergistic action of CA and EW increased the compound's bactericidal effectiveness. Amino acid metabolism is one of the most severely impacted pathways in the three strains. Catabolism was more advantageous than anabolism in these strains when treated in combination. This might be because the amino acid synthesis pathway is susceptible to unfavourable conditions like heat and acid (Wu et al., 2021). Additionally, several enzymatic activities involved in amino acid catabolism may be favoured in acidic environments due to their efficiency at producing alkaline molecules to compensate and consuming protons to compensate for low pH (Wang, Wu, & Yang, 2022). Decarboxylation is one of these reactions; under the catalysis of decarboxylase, free amino acids are transformed to amines to increase resistance to acidity and survival rate (Ferrario et al., 2014). Apart from the low pH, which necessitates the catalysis of amino acid enzymes, FAC results in additional amino acid depletion in the strain. For example, HOCl is highly powerful against sulphur-containing amino acids (Da Cruz Nizer, Inkovskiy, & Overhage, 2020), resulting in increased methionine reduction in strains. Because several amino acids, including alanine, proline, glycine, and glutamate, are natural osmotic regulators (Wiesenthal, Müller, Harder, & Hildebrandt, 2019, Wu et al., 2021), Due to the increased amino acid intake, there may be insufficient osmotic agents to maintain cytoplasmic osmotic pressure, resulting in the degradation of subcellular structures and potentially cell death.

After combination treatment, considerable succinic acid depletion was seen in all strains, suggesting that variable degrees of TCA cycle damage occurred, resulting in insufficient energy supply and cell death. Initially, glucose was an excellent source of carbon and energy for bacteria since it could be used in metabolic pathways for energy generation. As a glucose catabolism route, glycolysis may give precursors and energy for cellular biosynthesis (Doi, 2019). The decrease in ATP

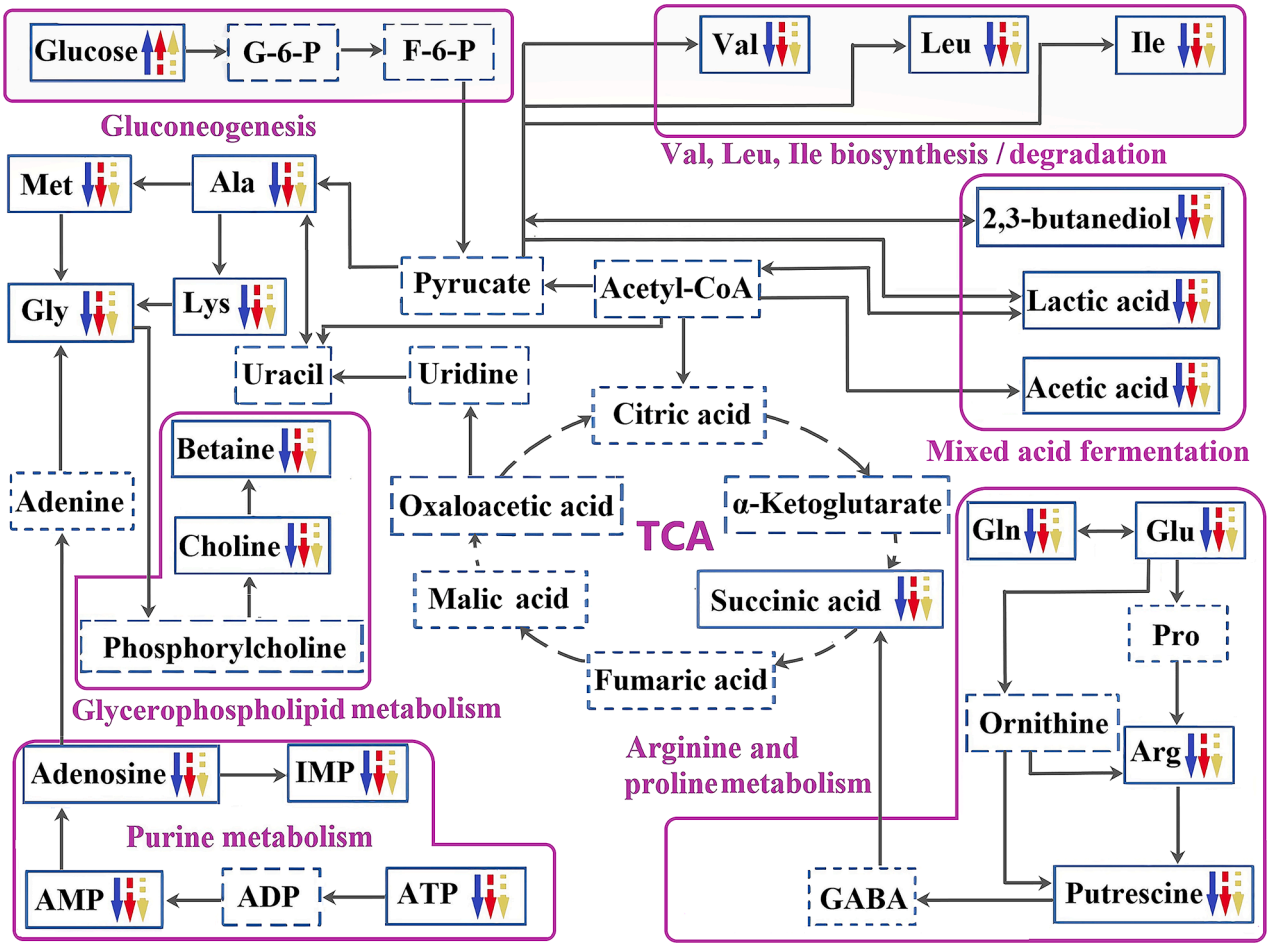

Fig. 7. Overview of metabolism disturbance affected by the combined treatment in three *Aeromonas* strains. Notes: The increase and decrease of metabolite changes in the 1 % citric acid + electrolysed water group compared with that in the deionised water group was represented by the upward and downward arrows next to the metabolite. Blue arrows: strain 1; Red arrows: strain 2; Yellow arrows: strain 3. The omitted TCA cycle was connected by a virtual arrow. Metabolites in the dotted box were not detected. The pathways significantly affected in the three strains were marked with purple boxes. (For interpretation of the references to colour in this figure legend, the reader is referred to the web version of this article.)

levels indicated that the combined treatment inhibited the energy supplementation of the metabolic pathway, resulting in a reduction of glucose utilisation rate in the three *Aeromonas* strains, which also explained why the glucose content of the combined treatment group was significantly higher than the that of the DW group. Since putrescine is involved in cell division and is used as a growth indicator for bacteria (Ye et al., 2012), the considerable decrease in putrescine levels showed that the combination treatment inhibited the growth of strains. Putrescine is a precursor to γ-aminobutyrate (GABA), which means that a reduction of putrescine will also decrease GABA. Because GABA may be converted to succinic acid by GABA shunt (Ravasz et al., 2017), its depletion may reduce succinic acid entering the TCA cycle. As a result, the TCA cycle becomes even more vulnerable.

Along with interfering with energy metabolism, the combined treatment also caused significant oxidative stress in bacteria strains due to the presence of EW in the combined treatment. Oxidative stress affects the intracellular redox equilibrium of glutathione disulphide redox couples, resulting in cytotoxicity (Murray, Messner, & Kowdley, 2012). Putrescine may have a role in reducing oxidative stress since Cao et al. (2021) reported that it indirectly increases the activity of alkyl-hydro peroxidase reductase, glutathione reductase, and hydroperoxides I via altering important adaptive response regulators. Thus, reactive oxygen species are eliminated, and the decreased form of intracellular redox pairs is restored. As a result, the reduced putrescine levels reported in all three strains may represent the decrease in anti-oxidative stress ability. Additionally, the similar trend in betaine levels amongst the three strains validated our findings. Betaine is a chemical partner that choline produces. It helps keep the cell structure intact and is considered an osmotic protection molecule (Gaucher et al., 2020). In the process of maintaining osmotic homeostasis, the decrease of betaine content leads to the reduction of the osmotic protection ability of bacterial strains and finally leads to bacterial death.

4. Conclusion

In conclusion, this study investigated the effects of three kinds of *Aeromonas* bacteria on metabolite profiles of barramundi fillets after combined treatment during cold storage. Three different *Aeromonas* species were isolated and identified from three different parts of spoilage barramundi. Microbial analysis data indicated that compared with DW, CA, and EW groups, the combination of CA and EW treatment had the most apparent antibacterial effect on the three kinds of *Aeromonas* bacteria, inducing a reduction of 1.64–1.69 log CFU/g. In addition, through fluorescence staining analysis, the combined treatment group significantly increased the adverse effects on the membrane integrity, which may be due to their specific action sites and action modes on the bacterial membrane, allowing CA and EW to attack the membrane in multiple dimensions. The three strains showed similar metabolic profiles with 36 specific metabolites. The combined treatment group significantly reduced the change of main metabolite content. Further studies

suggested that these changes may be due to interference and alteration of amino acid, energy, and carbohydrate metabolic pathways, observed in all three *Aeromonas* strains, but to varying degrees. This study indicated that the bactericidal mechanism of the antibacterial substance may be explained by the interference of the metabolic pathway, which provides guidance for post-treatment sanitisation, and extends the applicability of the NMR spectrum to SSO analysis in fish storage.

CRediT authorship contribution statement

Leijian Chen: Conceptualization, Methodology, Investigation, Software, Visualization, Writing – original draft, Writing – review & editing. **Xuan Li:** Investigation, Software, Visualization. **Xiaowei Lou:** Investigation, Methodology. **Weichen Shu:** Investigation. **Yaowen Hai:** Investigation. **Xiaokang Wen:** Investigation, Methodology. **Hongshun Yang:** Conceptualization, Funding acquisition, Project administration, Supervision, Writing – review & editing.

Declaration of Competing Interest

The authors declare that they have no known competing financial interests or personal relationships that could have appeared to influence the work reported in this paper.

Data availability

Data will be made available on request.

Acknowledgements

This study was funded by Singapore Ministry of Education Academic Research Fund Tier 1 (A-8000469-00-00) and an industry project from Shanghai ProfLeader Biotech Co., Ltd (A-0008416-00-00).

Appendix A. Supplementary material

Supplementary data to this article can be found online at https://doi.org/10.1016/j.foodres.2022.112046.

References

Anyasi, T., Jideani, A., Edokpayi, J., & Anokwuru, C. (2017). Application of organic acids in food preservation. In C. Vargas (Ed.), *Organic Acids: Characteristics, Properties, and Synthesis* (pp. 1–45). Essay, Nova Science Publishers, Inc.

Arslan, S., & Küçüksari, R. (2015). Phenotypic and genotypic virulence factors and antimicrobial resistance of motile *Aeromonas* spp. from fish and ground beef. *Journal of Food Safety, 35*(4), 551–559.

Batra, P., Mathur, P., & Misra, M. C. (2016). *Aeromonas* spp.: An emerging nosocomial pathogen. *Journal of Laboratory Physicians, 8*(1), 1–4.

Beaz-Hidalgo, R., Agüeria, D., Latif-Eugenín, F., Yeannes, M. I., & Figueras, M. J. (2015). Molecular characterisation of *Shewanella* and *Aeromonas* isolates associated with spoilage of common carp (*Cyprinus carpio*). *FEMS Microbiology Letters, 362*(1), 1–8.

Bushell, F. M., Tonner, P. D., Jabbari, S., Schmid, A. K., & Lund, P. A. (2019). Synergistic impacts of organic acids and pH on growth of *Pseudomonas aeruginosa*: A comparison of parametric and bayesian non-parametric methods to model growth. *Frontiers in Microbiology, 9*, 3196.

Cao, Y., Jiao, Y., Zhan, S., Liang, X., Li, Z., Chen, J., … Zheng, Z. (2021). Polyamine putrescine regulates oxidative stress and autophagy of hemocytes induced by lipopolysaccharides in pearl oyster *Pinctada fucata martensii*. *Frontiers in Physiology, 12*, Article 781324.

Chen, L., Wu, J., Li, Z., Liu, Q., Zhao, X., & Yang, H. (2019). Metabolomic analysis of energy regulated germination and sprouting of organic mung bean (*Vigna radiata*) using NMR spectroscopy. *Food Chemistry, 286*, 87–97.

Chen, L., Zhao, X., Wu, J., Liu, Q., Pang, X., & Yang, H. (2020). Metabolic characterisation of eight *Escherichia coli* strains including "big six" and acidic responses of selected strains revealed by NMR spectroscopy. *Food Microbiology, 88*, Article 103399.

Cho, G. L., & Ha, J. W. (2021). Synergistic effect of citric acid and xenon light for inactivating foodborne pathogens on spinach leaves. *Food Research International (Ottawa Ont.), 142*, Article 110210.

Culyba, M. J., & Van Tyne, D. (2021). Bacterial evolution during human infection: Adapt and live or adapt and die. *PLOS Pathogens, 17*(9), e1009872.

Da Cruz Nizer, W. S., Inkovskiy, V., & Overhage, J. (2020). Surviving reactive chlorine stress: Responses of gram-negative bacteria to hypochlorous acid. *Microorganisms, 8*(8), 1220.

Dewi, F. R., Stanley, R., Powell, S. M., & Burke, C. M. (2017). Application of electrolysed oxidising water as a sanitiser to extend the shelf-life of seafood products: A review. *Journal of Food Science and Technology, 54*(5), 1321–1332.

Doi, Y. (2019). Glycerol metabolism and its regulation in lactic acid bacteria. *Applied Microbiology and Biotechnology, 103*(13), 5079–5093.

Eliuz, E. (2020). Antimicrobial activity of citric acid against *Escherichia coli*, *Staphylococcus aureus* and *Candida albicans* as a sanitiser agent. *Eurasian Journal of Forest Science, 8*(3), 295–301.

FAO, 2012. The state of world fisheries and agriculture. Rome.

Ferrario, C., Borgo, F., de las Rivas, B., Muñoz, R., Ricci, G., & Fortina, M. G. (2014). Sequencing, characterisation, and gene expression analysis of the histidine decarboxylase gene cluster of *Morganella morganii*. *Current Microbiology, 68*(3), 404–411.

Gaucher, F., Rabah, H., Kponouglo, K., Bonnassie, S., Pottier, S., Dolivet, A., … Jan, G. (2020). Intracellular osmoprotectant concentrations determine *Propionibacterium freudenreichii* survival during drying. *Applied Microbiology and Biotechnology, 104*(7), 3145–3156.

Hati, S., Mandal, S., Minz, P. S., Vij, S., Khetra, Y., Singh, B. P., & Yadav, D. (2012). Electrolysed oxidised water (EOW): Non-thermal approach for decontamination of food borne microorganisms in food industry. *Food and Nutrition Sciences, 03*(06), 760–768.

Hoel, S., Vadstein, O., & Jakobsen, A. N. (2019). The significance of mesophilic Aeromonas spp. in minimally processed ready-to-eat Seafood. *Microorganisms, 7*(3), 91.

Iulietto, M., Sechi, P., Borgogni, E., & Cenci-Goga, B. (2015). Meat Spoilage: A critical review of a neglected alteration due to ropy slime producing bacteria. *Italian Journal of Animal Science, 14*(3), 4011.

Jakobsen, A., Shumilina, E., Lied, H., & Hoel, S. (2020). Growth and spoilage metabolites production of a mesophilic *Aeromonas salmonicida* strain in Atlantic salmon (*Salmo salar* L.) during cold storage in modified atmosphere. *Journal of Applied Microbiology, 129*(4), 935–946.

Kim, H. J., Tango, C. N., Chelliah, R., & Oh, D. H. (2019). Sanitisation efficacy of slightly acidic electrolysed water against pure cultures of *Escherichia coli*, *Salmonella enterica*, *Typhimurium*, *Staphylococcus aureus* and *Bacillus cereus* spores, in comparison with different water hardness. *Scientific Reports, 9*(1), 4348.

Koromyslova, A., White, P., & Hansman, G. (2015). Treatment of norovirus particles with citrate. *Virology, 485*, 199–204.

Liu, L., Lan, W., Wang, Y., & Xie, J. (2022). Antibacterial activity and mechanism of slightly acidic electrolysed water against *Shewanella putrefaciens* and *Staphylococcus saprophytic*. *Biochemical and Biophysical Research Communications, 592*, 44–50.

Lou, X., Zhai, D., & Yang, H. (2021). Changes of metabolite profiles of fish models inoculated with *Shewanella Baltica* during spoilage. *Food Control, 123*, Article 107697.

Lund, P. A., De Biase, D., Liran, O., Scheler, O., Mira, N. P., Cetecioglu, Z., … O'Byrne, C. (2020). Understanding how microorganisms respond to acid pH is central to their control and successful exploitation. *Frontiers in microbiology, 11*, Article 556140.

Manjul, A. S., & Shirkot, P. (2018). 16S rRNA gene sequencing for bacterial identification of pullulanase synthesising thermophilic bacteria contributing to big data. *International Journal of Chemical Studies, 6*(2), 2769–2773.

Marchetti, L., Pellati, F., Benvenuti, S., & Bertelli, D. (2019). Use of ^{1}H NMR to detect the percentage of pure fruit juices in blends. *Molecules, 24*(14), 2592.

McDermott, A., Whyte, P., Brunton, N., Lyng, J., Fagan, J., & Bolton, D. (2018). The effect of organic acid and sodium chloride dips on the shelf-life of refrigerated Irish brown crab (*Cancer pagurus*) meat. *LWT-Food Science and Technology, 98*, 141–147.

Meireles, A., Giaouris, E., & Simões, M. (2016). Alternative disinfection methods to chlorine for use in the fresh-cut industry. *Food Research International (Ottawa, Ont.), 82*, 71–85.

Murray, K., Messner, D., & Kowdley, K. (2012). Mechanisms of hepatocyte detoxification. In H. M. Said, & F. K. Ghishan (Eds.), *Physiology of the Gastrointestinal Tract* (pp. 1507–1527). Essay, Academic Press.

Rahman, S., Jin, Y., & Oh, D. (2011). Combination treatment of alkaline electrolysed water and citric acid with mild heat to ensure microbial safety, shelf-life and sensory quality of shredded carrots. *Food Microbiology, 28*(3), 484–491.

Ravasz, D., Kacso, G., Fodor, V., Horvath, K., Adam-Vizi, V., & Chinopoulos, C. (2017). Catabolism of GABA, succinic semialdehyde or gamma-hydroxybutyrate through the GABA shunt impair mitochondrial substrate-level phosphorylation. *Neurochemistry International, 109*, 41–53.

Rosenberg, M., Azevedo, N., & Ivask, A. (2019). Propidium iodide staining underestimates viability of adherent bacterial cells. *Scientific Reports, 9*(1), 6483.

Schieber, M., & Chandel, N. S. (2014). ROS function in redox signalling and oxidative stress. *Current Biology: CB, 24*(10), R453–R462.

Shumilina, E., Ciampa, A., Capozzi, F., Rustad, T., & Dikiy, A. (2015). NMR approach for monitoring post-mortem changes in Atlantic salmon fillets stored at 0 and 4 °C. *Food Chemistry, 184*, 12–22.

Stratford, M., Nebe-von-Caron, G., Steels, H., Novodvorska, M., Ueckert, J., & Archer, D. (2013). Weak-acid preservatives: pH and proton movements in the yeast *Saccharomyces cerevisiae*. *International Journal of Food Microbiology, 161*(3), 164–171.

Tango, C., Mansur, A., & Oh, D. (2015). Fumaric acid and slightly acidic electrolysed water inactivate gram positive and gram negative foodborne pathogens. *Microorganisms, 3*(1), 34–46.

Truong, B. Q., Buckow, R., Nguyen, M. H., & Nguyen, H. T. (2021). High pressure thermal sterilisation of barramundi (*Lates calcarifer*) muscles in brine: Effects on

selected physicochemical properties. *Journal of Food Processing and Preservation, 45*(6), e15523.
Wang, Y., Wu, J., & Yang, H. (2022). Comparison of the metabolic responses of eight *Escherichia coli* strains including the "big six" in pea sprouts to low concentration electrolysed water by NMR spectroscopy. *Food Control, 131*, Article 108458.
Wiesenthal, A. A., Müller, C., Harder, K., & Hildebrandt, J. P. (2019). Alanine, proline and urea are major organic osmolytes in the snail *Theodoxus fluviatilis* under hyperosmotic stress. *Journal of Experimental Biology, 222*(Pt 3), jeb193557.
Wood, J. M. (2015). Bacterial responses to osmotic challenges. *The Journal of General Physiology, 145*(5), 381–388.
Wu, J., Zhao, L., Lai, S., & Yang, H. (2021). NMR-based metabolomic investigation of antimicrobial mechanism of electrolysed water combined with moderate heat treatment against *Listeria monocytogenes* on salmon. *Food Control, 125*, Article 107974.
Wu, Y., Shi, Y. G., Zeng, L. Y., Pan, Y., Huang, X. Y., Bian, L. Q., … Zhang, J. (2019). Evaluation of antibacterial and anti-biofilm properties of kojic acid against five food-related bacteria and related subcellular mechanisms of bacterial inactivation. *Food Science and Technology International, 25*(1), 3–15.
Ye, Y., Zhang, L., Hao, F., Zhang, J., Wang, Y., & Tang, H. (2012). Global metabolomic responses of *Escherichia coli* to heat stress. *Journal of Proteome Research, 11*(4), 2559–2566.
Yemmireddy, V., Cason, C., Moreira, J., & Adhikari, A. (2020). Effect of pecan variety and the method of extraction on the antimicrobial activity of pecan shell extracts against different foodborne pathogens and their efficacy on food matrices. *Food Control, 112*, Article 107098.
Yoshioka, T., Konno, Y., & Konno, K. (2019). Below-zero storage of fish to suppress loss of freshness. *Fisheries Science, 85*(3), 601–609.
Zhao, D., Lyu, F., Liu, S., Zhang, J., Ding, Y., Chen, W., & Zhou, X. (2017). Involvement of bacterial quorum sensing signals in spoilage potential of *Aeromonas veronii* isolated from fermented surimi. *Journal of Food Biochemistry, 42*(2), e12487.
Zhao, L., Zhao, M. Y., Phey, C. P., & Yang, H. (2019). Efficacy of low concentration acidic electrolysed water and levulinic acid combination on fresh organic lettuce (*Lactuca sativa var. Crispa L.*) and its antimicrobial mechanism. *Food Control, 101*, 241–250.
Zhao, L., Zhao, X., Wu, J. E., Lou, X., & Yang, H. (2019). Comparison of metabolic response between the planktonic and air-dried *Escherichia coli* to electrolysed water combined with ultrasound by ^{1}H NMR spectroscopy. *Food Research International (Ottawa Ont.), 125*, Article 108607.
Zhao, X., Wu, J. E., Chen, L., & Yang, H. (2019). Effect of vacuum impregnated fish gelatin and grape seed extract on metabolite profiles of tilapia (*Oreochromis niloticus*) fillets during storage. *Food Chemistry, 293*, 418–428.